

# A statistical method for computing BOLD activations in multi-echo time fMRI data sets and identifying likely non-BOLD task related signal change

A. S. Nencka<sup>1</sup>, D. L. Shefchik<sup>1</sup>, J. S. Hyde<sup>1</sup>, A. Jesmanowicz<sup>1</sup>, and D. B. Rowe<sup>2</sup>

<sup>1</sup>Department of Biophysics, Medical College of Wisconsin, Milwaukee, WI, United States, <sup>2</sup>Department of Mathematics, Statistics and Computer Science, Marquette University, Milwaukee, WI, United States

## Introduction:

Multi-echo-time echo planar image acquisitions allow for the consideration of BOLD related  $T_2^*$  decay. Studies which have included single-shot, multi-echo acquisitions to calculate  $T_2^*$  have been shown to yield activations which are appropriately localized when compared to proton spin density images calculated from the same  $T_2^*$  weighted images (1), allowing the separation of BOLD  $T_2^*$  effects from other effects which arise in the proton spin density images. However, such pulse sequences require the acquisition of additional data in each shot, reducing the available slice coverage for a given TR. In this abstract, we present a method for the statistical analysis of multi-echo time fMRI data, and apply it to data acquired in a pulse sequence where the echo time is shifted by 20 ms for alternating TRs, thereby allowing the same slice coverage as standard, single echo data acquisitions.

## Theory:

BOLD contrast relies upon a change in the  $T_2^*$  decay rate of blood as oxygenation changes during cortical activation. Previous studies have found that the  $T_2^*$  of blood changes from 45.33 ms in rest to 46.56 ms during task at 3.0 T (2). Thus, different BOLD contrast is expected with different echo times, as seen in Figure 1. True BOLD activations are expected to exhibit changes in BOLD contrast that corresponds to this theoretical result, while other potentially task related signal not of interest may exhibit a different echo-time-dependent contrast pattern.

A general linear model was developed to be applied to multi-echo time data. For the case of two echo times, the model includes a six column design matrix, including one column for the baseline signal of the first echo time ( $TE_1$ ),

one column for the baseline signal of the second echo time ( $TE_2$ ), one column for the linear trend of  $TE_1$  data, one column for the linear trend of  $TE_2$  data, one column for the task related response to  $TE_1$ , and one column for the task related response to  $TE_2$ . The voxel-wise model is shown in Equation 1, where  $n$  is the number of time points,  $y$  is a vector of the observed time series,  $\beta$  is a vector of unknown regression coefficients, and  $\Sigma$  is a vector of normally distributed noise ( $\Sigma \sim N(0, I^2)$ ).

## Methods:

Functional neuroimages were acquired in a subject, in concordance with the procedures of the institutional review board. The subject performed a visually-cued block-designed bilateral finger-tapping task with 7 epochs of 16 seconds rest, 16 seconds task, followed by 16 seconds of rest. Scanning parameters included  $TE_1=47.0$  ms,  $TE_2=27.0$  ms,  $TR=2$  s, flip angle=90 degrees, acquisition matrix=64x64, field of view=24 cm, slice thickness=5 mm, 8 channel head receiver, on a 3.0T General Electric Signa LX imager. Activations were computed to find voxels active in only  $TE_1$  data, only  $TE_2$  data, and both  $TE_1$  and  $TE_2$  data. Chi-squared statistics were computed from the model through a likelihood ratio test, and were thresholded with an  $\alpha=0.05$ , Bonferroni adjusted threshold. Contrasts of  $C_1=(0\ 0\ 0\ 0\ 1)$ ,  $C_2=(0\ 0\ 0\ 0\ 1\ 0)$ , and  $C_3=(0\ 0\ 0\ 1\ 1)$  were utilized to determine voxels which were active in the data acquired with the second echo time, first echo time, and either echo time, respectively.

## Results:

Activations found with contrasts  $C_1$ ,  $C_2$ , and  $C_3$  for a representative slice are shown in Figures 2, 3 and 4. The different echo times are sensitive to different voxels, with the longer echo time yielding more activations with its increased  $T_2^*$  weighting, and the case of considering both echo times simultaneously yielding the most activations. To consider the  $T_2^*$  dependence of the observed activations, the ratio of  $\beta_4$  to  $\beta_5$  is shown for the active voxels with constraints  $C_1$ ,  $C_2$ , and  $C_3$  for the same slice in Figures 5, 6 and 7. As indicated in Figure 1, the expected BOLD response should yield a ratio of about 1.15.

## Discussion:

The ratio of task related functional responses to different echo times can be used to identify voxels which exhibit expected functional BOLD contrast. In support of this methodology, Figures 5 and 7 illustrate that clear false positives outside of the brain can be excluded as the ratio is much less than one, while the expected BOLD ratio is slightly greater than one. Additionally, voxels on the periphery of activated regions exhibit TE dependent ratios which are markedly different from the expected BOLD ratio, suggesting that these voxels may be exhibiting a task related contrast which differs from the expected BOLD contrast, perhaps associated with varying partial volume effects from task related motion.

**References:** (1)NIMG 16:985-992 (2) MRM 53:808-816

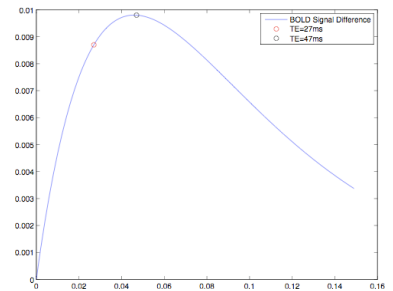


Fig. 1: BOLD Response Curve

$$\begin{bmatrix} y_1 \\ y_2 \\ y_3 \\ y_4 \\ y_5 \\ y_6 \\ \vdots \\ y_{n-1} \\ y_n \end{bmatrix} = \begin{bmatrix} 1 & 0 & -n/2 & 0 & -1 & 0 \\ 0 & 1 & 0 & -n/2 & 0 & -1 \\ 1 & 0 & -n/2+1 & 0 & -1 & 0 \\ 0 & 1 & 0 & -n/2+1 & 0 & -1 \\ 1 & 0 & -n/2+2 & 0 & 1 & 0 \\ 0 & 1 & 0 & -n/2+2 & 0 & 1 \\ \vdots & \vdots & \vdots & \vdots & \vdots & \vdots \\ 1 & 0 & n/2 & 0 & -1 & 0 \\ 0 & 1 & 0 & n/2 & 0 & -1 \end{bmatrix} \begin{bmatrix} \beta_1 \\ \beta_2 \\ \beta_3 \\ \beta_4 \\ \beta_5 \\ \beta_6 \end{bmatrix} + \begin{bmatrix} \epsilon_1 \\ \epsilon_2 \\ \epsilon_3 \\ \epsilon_4 \\ \epsilon_5 \\ \epsilon_6 \\ \vdots \\ \epsilon_{n-1} \\ \epsilon_n \end{bmatrix}$$

Eqn. 1: Proposed Multi-TE Model

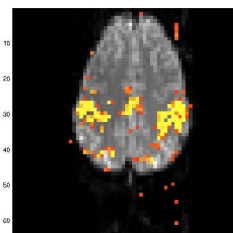


Fig. 2:  $C_1$  Activations

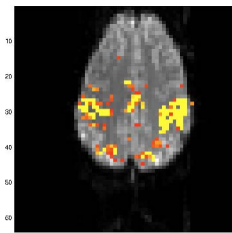


Fig. 3:  $C_2$  Activations

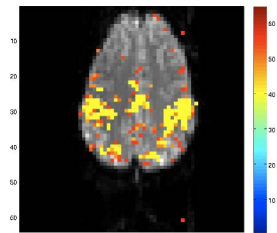


Fig. 4:  $C_3$  Activations

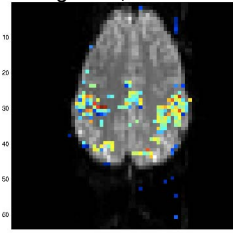


Fig. 5:  $\beta_4/\beta_5$  for  $C_1$  Activations

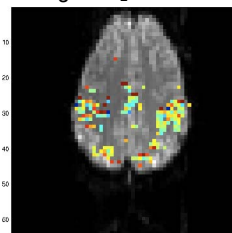


Fig. 6:  $\beta_4/\beta_5$  for  $C_2$  Activations

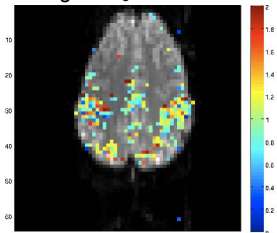


Fig. 7:  $\beta_4/\beta_5$  for  $C_3$  Activations